

Electronic Supplementary Information

## **An ultra-sensitive gas sensor based on two-dimensional manganese porphyrin monolayer**

Ze-Wen Hao,<sup>a‡</sup> Mi-Mi Dong,<sup>a‡</sup> Rui-Qin Zhang,<sup>b</sup> Chuan-Kui Wang,<sup>a\*</sup> Xiao-Xiao Fu<sup>a\*</sup>

<sup>a</sup> *Shandong Key Laboratory of Medical Physics and Image Processing & Shandong Provincial Engineering and Technical Center of Light Manipulations, School of Physics and Electronics, Shandong Normal University, Jinan 250358, China*

<sup>b</sup> *Department of Physics, City University of Hong Kong, Hong Kong Special Administrative Region*

‡ These authors contributed equally to this work

\* E-mail: ckwang@sdsu.edu.cn; fuxiaoxiao@sdsu.edu.cn

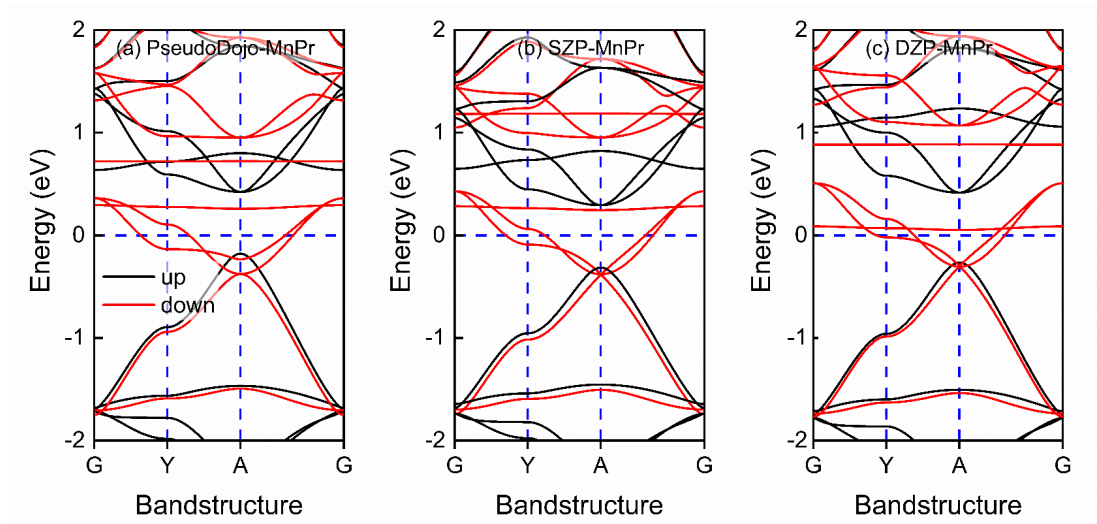


Fig. S1 Band structures of pure 2DMnPr calculated by PseudoDojo-Medium, SZP and DZP basis set.

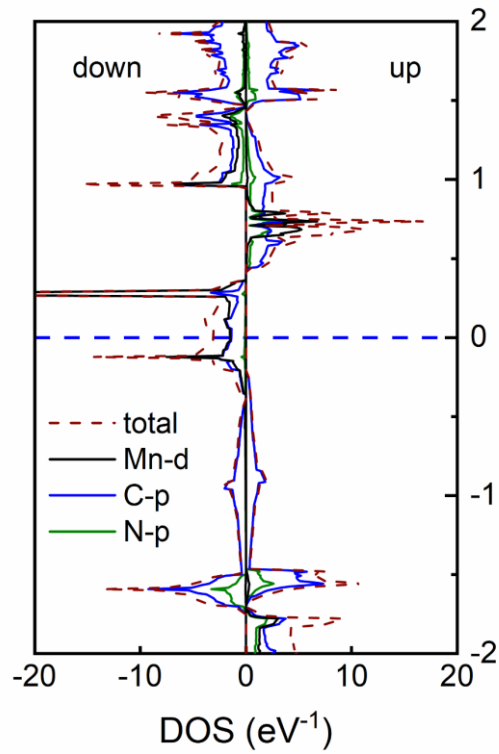
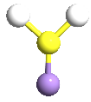
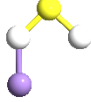
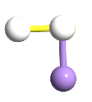
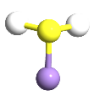
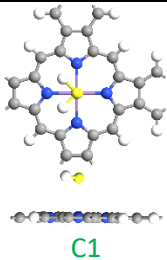
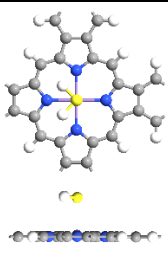
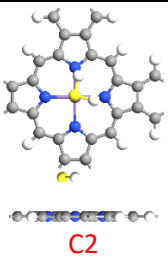
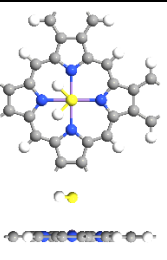




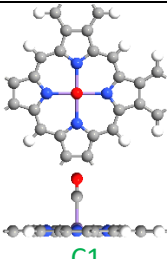
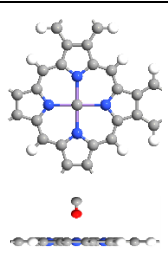
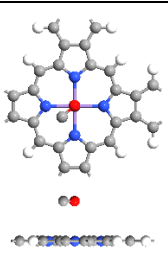
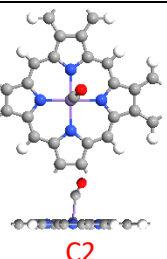



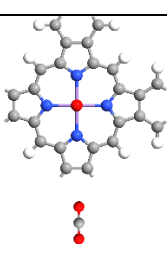
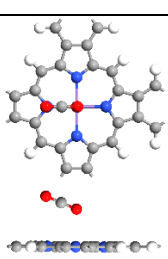
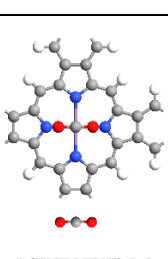
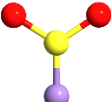

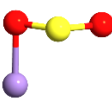
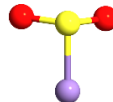
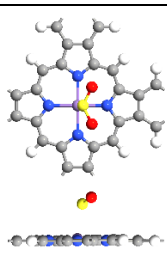
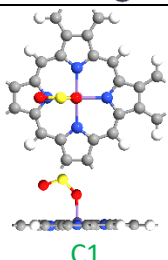
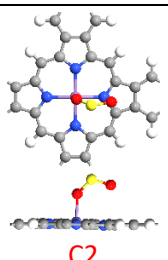
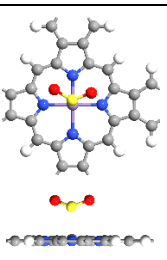


Fig. S2 Density of states (DOS) of 2DMnPr.

H <sub>2</sub> S	initial structures				
	optimized structures	 C1		 C2	
	Energy (eV)	-8481.52	-8481.55	-8481.59	-8481.57
CO	initial structures				
	optimized structures	 C1			 C2
	Energy (eV)	-8762.30	-8761.88	-8761.89	-8762.32
CO <sub>2</sub>	initial structures				
	optimized structures	 C1=C2	 C1=C2		
	Energy (eV)	-9214.10	-9214.19	-9214.09	
SO <sub>2</sub>	initial structures				
	optimized structures	 C1	 C1	 C2	
	Energy (eV)	-9349.85	-9350.15	-9350.17	-9349.92



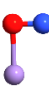

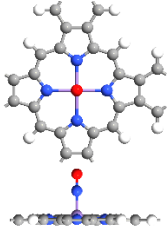
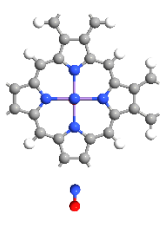
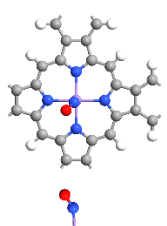
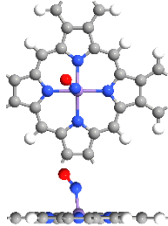


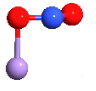
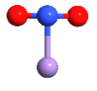
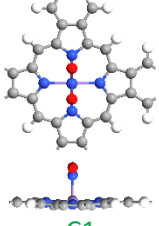
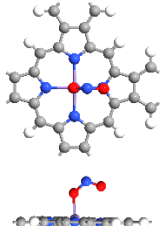
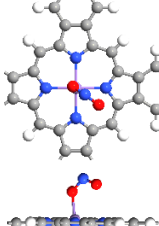
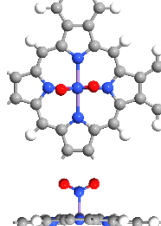
NO	initial structures				
	optimized structures	 C1			 C2
	Energy (eV)	-8880.37	-8878.80	-8880.48	-8880.48
NO <sub>2</sub>	initial structures				
	optimized structures	 C1			
	Energy (eV)	-9329.82	-9329.81	-9329.87	-9329.87

Fig. S3 Possible structures of adsorption gas molecules on central Mn atom.

H <sub>2</sub> S	initial structures				
	optimized structures				
	Energy (eV)	-8481.54	-8481.23	-8481.30	-8481.58
CO	initial structures				
	optimized structures				
	Energy (eV)	-8762.32	-8761.87	-8761.93	-8761.92
CO <sub>2</sub>	initial structures				
	optimized structures				
	Energy (eV)	-9214.07	-9214.19	-9214.18	
SO <sub>2</sub>	initial structures				
	optimized structures				
	Energy (eV)	-9349.67	-9350.08	-9349.75	-9349.97





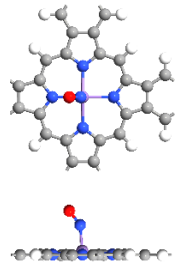
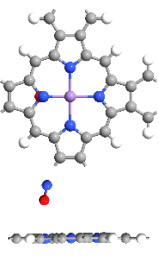
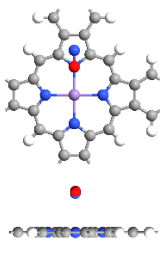
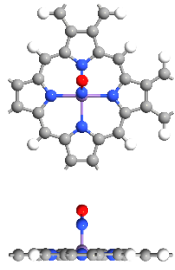

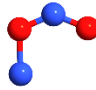
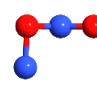

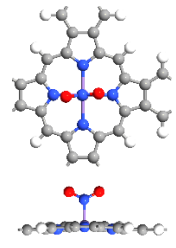
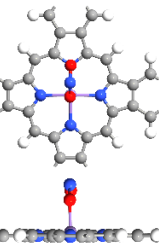
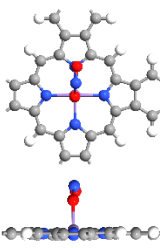
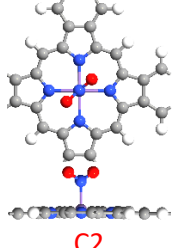
NO	initial structures				
	optimized structures				
	Energy (eV)	-8880.45	-8878.66	-8878.71	-8880.48
NO <sub>2</sub>	initial structures				
	optimized structures				
	Energy (eV)	-9329.91	-9329.83	-9329.86	-9329.99

Fig. S4 Possible structures of adsorption gas molecules on N atom.

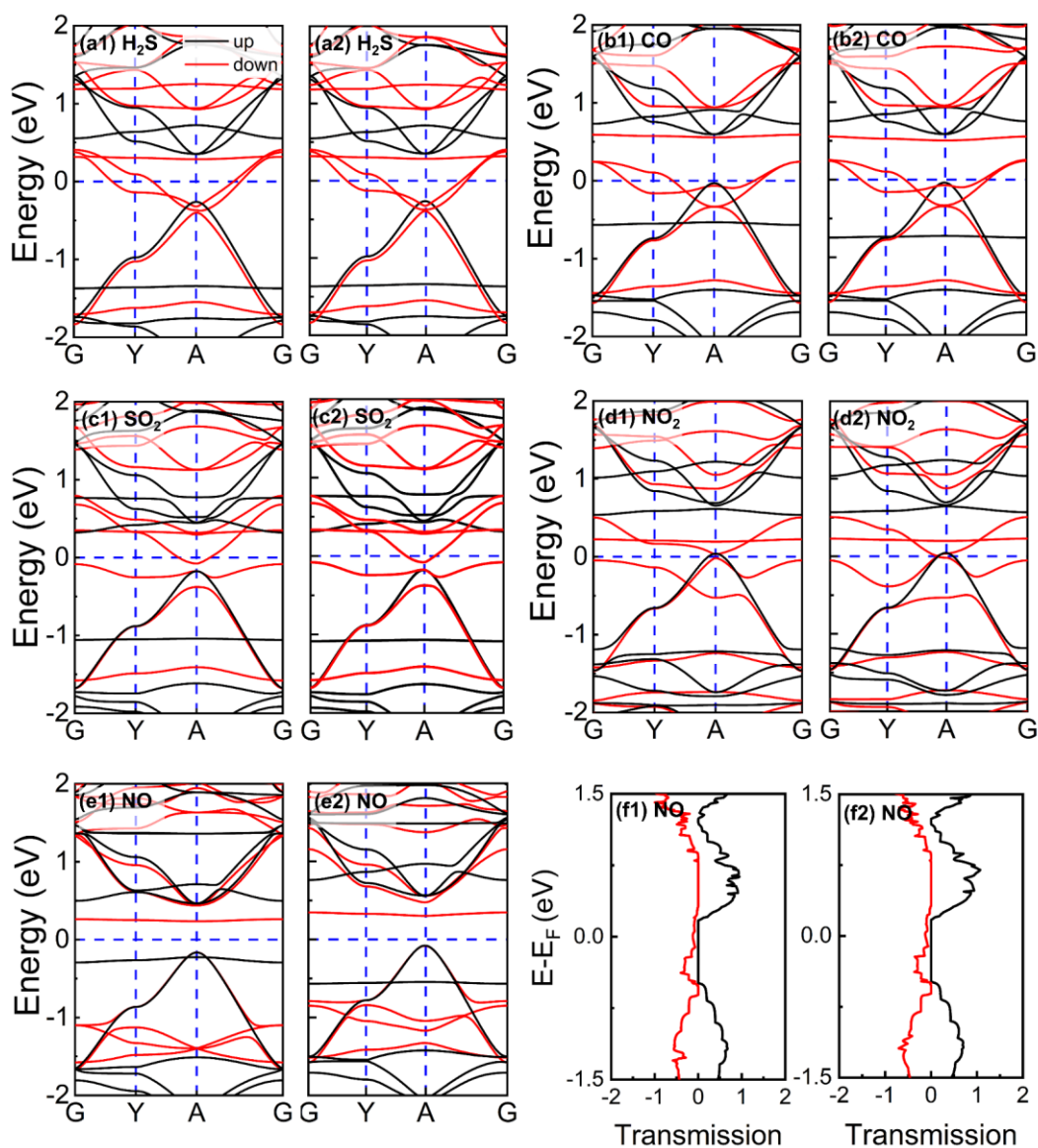


Fig. S5 (a1)-(e1) The band structures of the adsorption configurations used in the paper; (a2)-(e2) the band structures of the most stable adsorption configurations; (f1) and (f2) are the transmission spectra of the adsorbed NO configuration in the paper and the most stable adsorption configuration, respectively.

Fig. S3 shows the gas molecules adsorbed on the central Mn atom with different initial configurations and optimized stable configurations. Due to the high electronegativity of N atom, it is also considered as a possible adsorption site to adsorb gas molecules, as shown in Fig. S4. For the optimized configurations of the gas molecules on the N atom, one case is that the gas molecules stay on the N atom with

high total energy, meaning unstable configurations; the other is that the gas molecules move towards the central Mn atom, similar to those in Fig. S3. That means the central Mn atom is an ideal adsorption site for the gas molecules. The configuration we chose in the paper is marked by green (C1), and the energy favorable configuration is marked by red (C2). As shown in Fig. S3, the energy favorable configuration of CO<sub>2</sub> system is the one selected in the paper. There is little difference in the total energy between C1 and C2 configurations for the H<sub>2</sub>S, CO, SO<sub>2</sub>, NO<sub>2</sub> and NO adsorbed systems, and thus has little effect on the adsorption energy. As for the adsorption distance, most of C1 and C2 of the adsorption systems are the same, a few have differences about 0.01 Å between C1 and C2 configurations. We expect that the slight difference in adsorption energy and adsorption distance has little effect on the electronic properties. To confirm this, we have compared the band structures of the C1 and C2 in Fig. S4. For most of the adsorption systems, the band structures of C1 and C2 are almost undifferentiated. Only for the NO adsorption system, a flat spin-down band below the Fermi level moves down by 0.25 eV in C2. In order to further verify the effect of this flat band on the transport properties of the NO sensor, we calculate the transmission spectra under zero bias of these two configurations (see Fig. S5(f1) and Fig. S5(f2)). It can be clearly seen that the transmission spectra of the C1 configuration are similar to that of the C2, which indicates the effect of that flat spin-down band on transport properties of NO adsorption system can be neglected. Thus, the configurations we chose in the paper has little effect on the main conclusions of gas sensitivity based on the transmission characteristics. Besides, the configurations of gas molecules used in the paper have better spatial symmetry. So, it is meaningful to choose the stable configuration to prove the gas sensitivity of 2DMnPr.



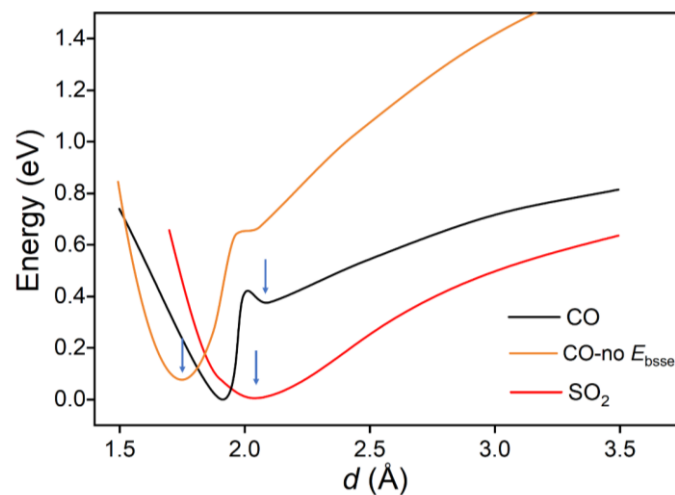


Fig. S6 The interaction energy with reference to the global minimum energy of the CO and  $SO_2$  adsorption systems as a function of the distance between Mn atom of 2DMnPr and the adatom of the gas molecules. The blue arrows denote the stable adsorption distance of the systems.

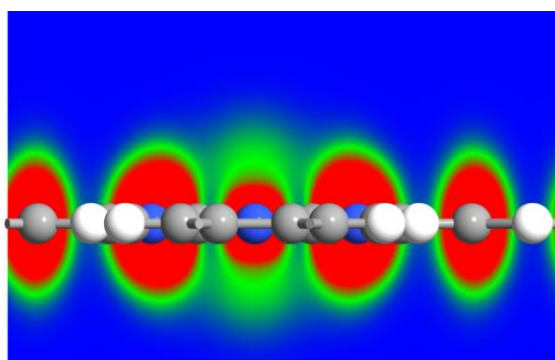


Fig. S7 Electron localization function of the 2DMnPr monolayer.

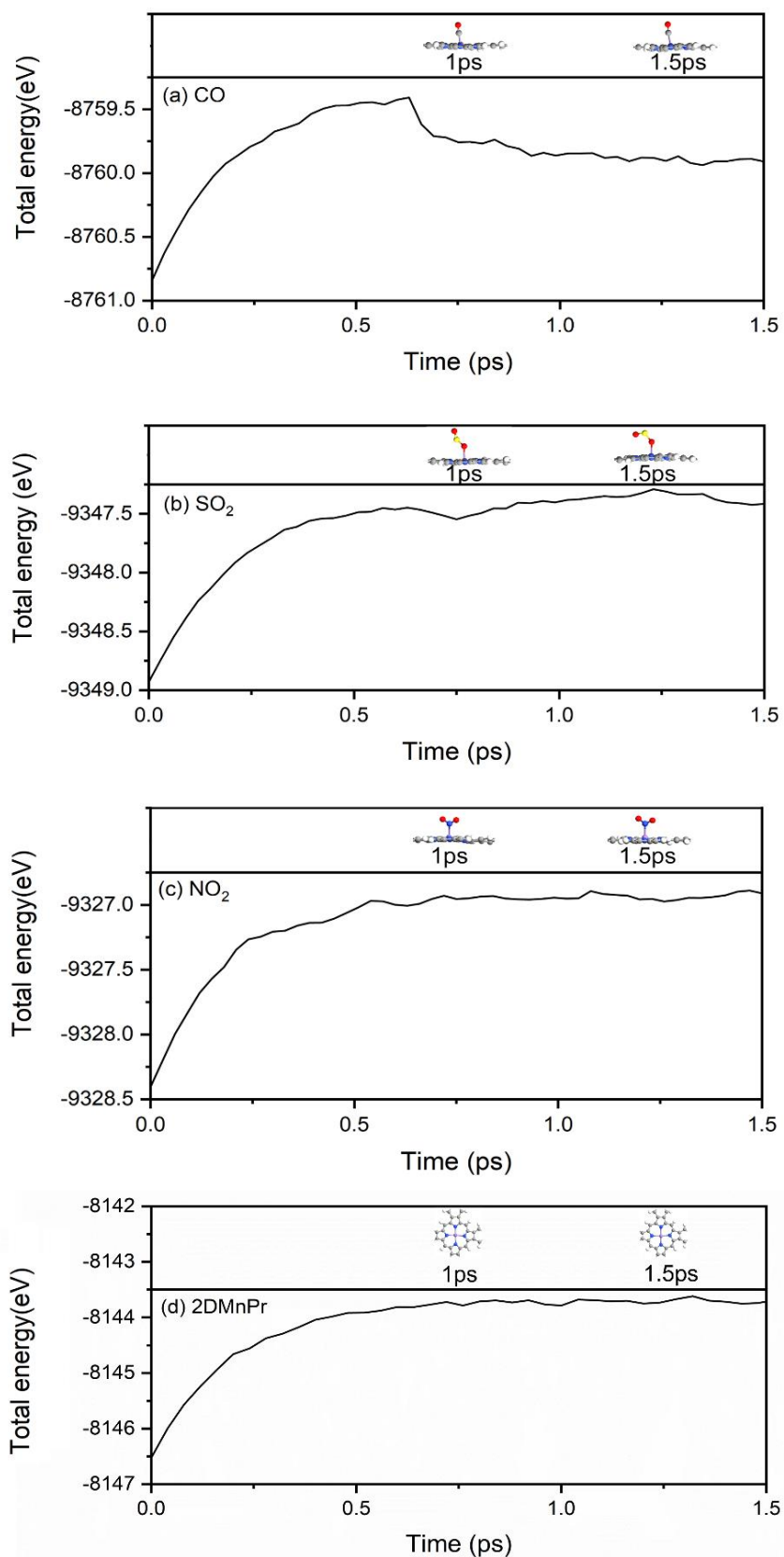


Fig. S8 (a)-(c) Molecular dynamics calculation of CO/SO<sub>2</sub>/NO<sub>2</sub>-2DMnPr systems at 300 K for 1.5 ps with 1fs time step, (d) the 2DMnPr at 600k for 1.5 ps with 1fs time step.

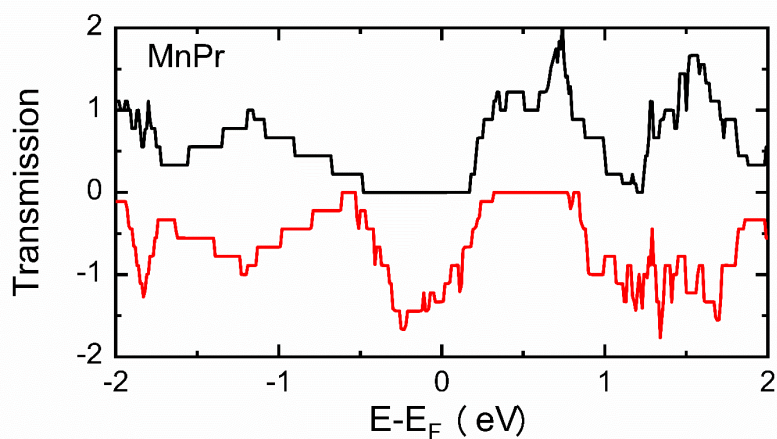


Fig. S9 Transmission spectra under zero bias of the 2DMnPr monolayer.

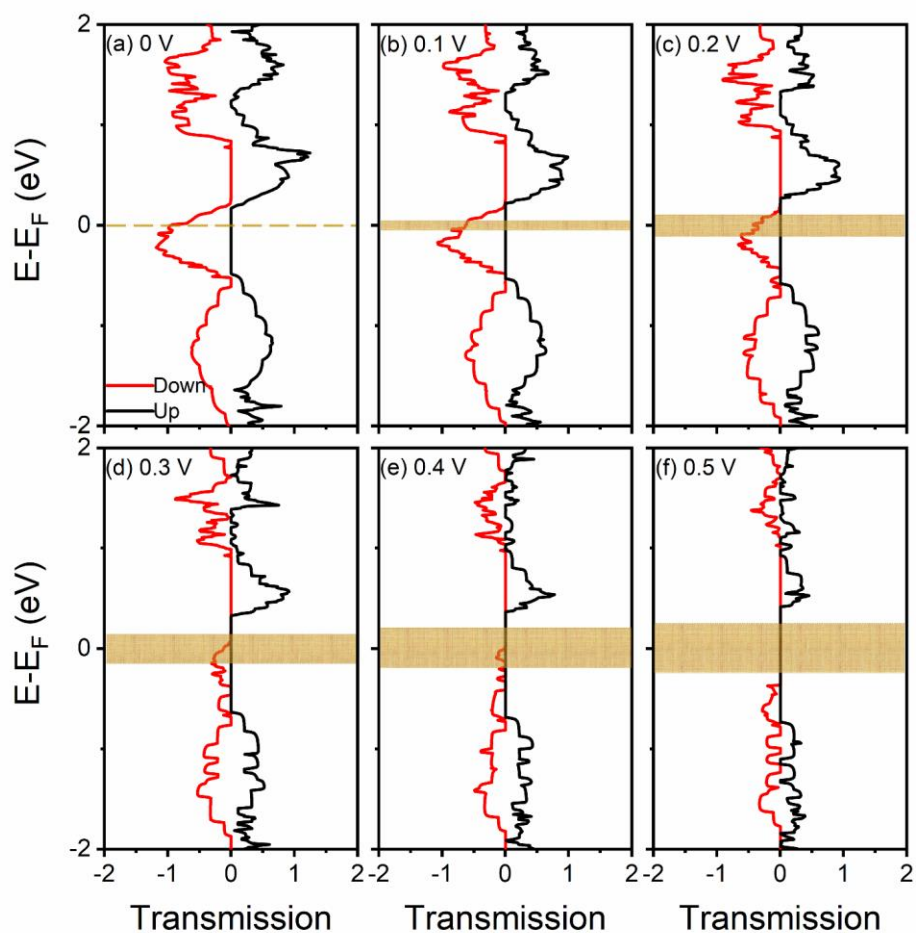


Fig. S10 (a)-(f) The transmission spectra of the CO adsorption system with bias ranging from 0 V to 0.5V. The black and the red lines represent spin-up and spin-down, respectively. The yellow color box represents the bias window.

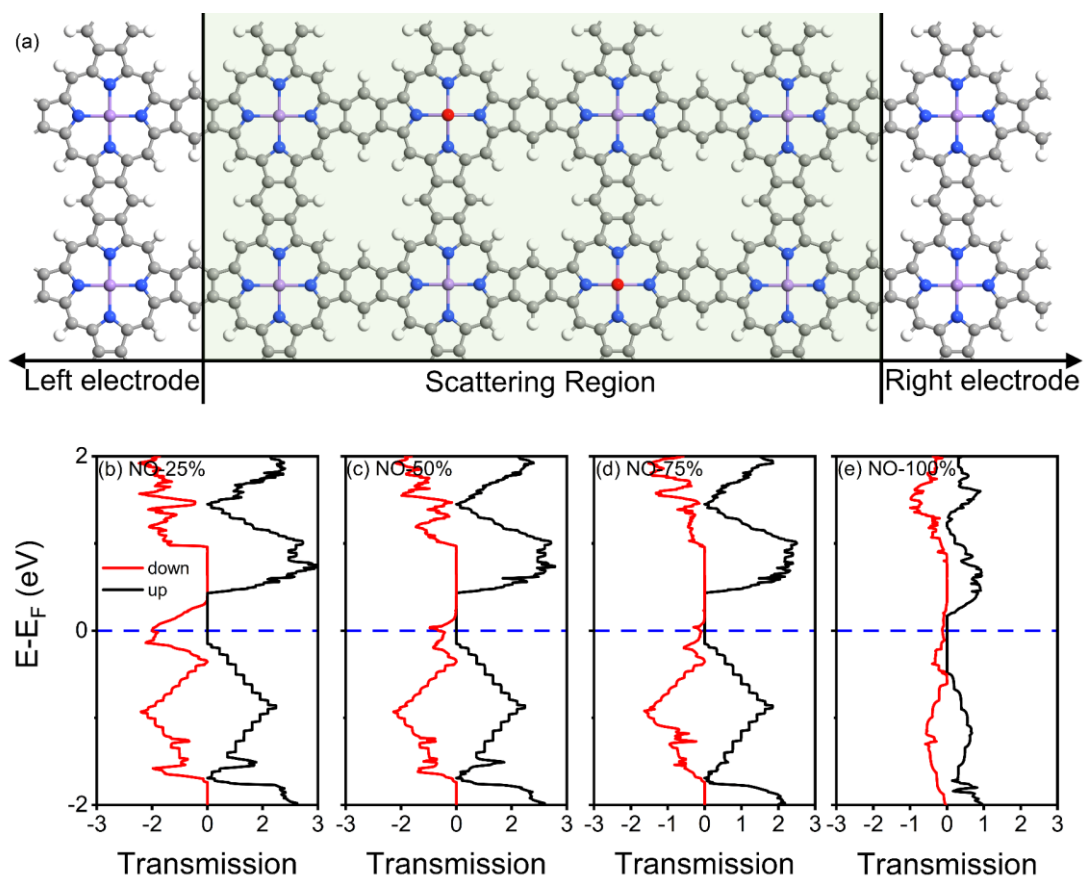


Fig. S11 (a) Schematic diagram of NO gas adsorption device model with 50% Mn atomic coverage; (b)-(d) the transmission spectra of NO adsorption system with gas coverage of 25%, 50%, 75% and 100%, respectively.